Journal of Materials Chemistry

PAPER

Low loss photopatternable matrix materials for LWIR-metamaterial applications†

Roger D. Rasberry,[a] Yun-Ju Lee,[a] James C. Ginn,[ab] Paul F. Hines,[a] Christian L. Arrington,[a] Andrea E. Sanchez,[a] Michael T. Brumbach,[a] Paul G. Clem,[a] David W. Peters,[a] Michael B. Sinclair[a] and Shawn M. Dirk*[a]

Transparent matrix materials with low-loss and low-permittivity are an important component of integrated optical devices including filters, lenses, and novel metamaterials. Many of the structural matrix materials that are currently utilized at visible and near-infrared wavelengths, such as solution deposited, high-k dielectrics and commercial photoresists, exhibit vibrational absorption bands in the 8–12 μm spectral range which represents a significant challenge to developing transmissive, three-dimensional (3D) metamaterials operating in the long wavelength infrared (LWIR) spectral region. In this paper, we present new, low loss photopatternable polymer dielectrics as well-suited matrix materials for fabricating LWIR-metamaterials. These materials are synthesized by partially hydrogenating polynorbornene to varying degrees followed by a thiol-ene coupling reaction to cross-link the remaining olefin groups. After cross-linking, the olefin LWIR-absorption band is minimized and the glass transition temperature (T_g) of the material increases. Thick layers of the polymer (>3 μm), which acts as a negative photoresist, can be deposited easily using a spin coating technique to develop planarizing layers with photopatternable vias. A demonstration on the low loss nature of the polymer dielectrics was carried out by incorporating the polymer into an all-dielectric, infrared metamaterial. Thus, the material is ideal for both lithography and fabrication of 3D metamaterial structures operating in the LWIR spectral region.

Introduction

Metamaterials are artificially-structured resonant materials which manipulate the flow of electromagnetic energy to afford properties that are not typically found in naturally occurring materials.[1,2] For example, electromagnetic cloaking has been demonstrated at microwave frequencies and it is theoretically plausible that the first perfect lens will be constructed entirely of negative refractive index metamaterials.[3,4] So far, most metamaterials have been fabricated using metallic unit cell structures embedded in a dielectric matrix.[5] Though well-suited for low frequency applications (*e.g.* <1 THz), metals are besieged by high ohmic losses at high frequencies which presents a tremendous challenge as we move toward implementing metamaterials that operate at optical frequencies (visible and infrared).[6–12] Researchers have sought to compensate for ohmic loss with

alternative strategies for reducing metamaterial absorption that include the development of gain media and protocols for fabricating 3D metamaterials supporting volumetric energy flow.[13–16] One straight-forward way to drastically reduce metamaterial loss is to remove the metal completely and replace it with a very low loss dielectric resonator.[17] In this case, the loss contribution of the dielectric matrix material begins to be appreciable compared to the low loss dielectric resonator.

The primary components of an all-dielectric metamaterial are two dielectric resonators which generate negative permittivity ($-\varepsilon_{\mathrm{eff}}$) and negative permeability ($-\mu_{\mathrm{eff}}$) simultaneously.[18–23] In this design, the importance of the dielectric matrix appears minimal; serving only as a support for the dielectric resonators. However, metamaterial fabrication is not trivial and the resonant fields of the dielectric resonators which extend into the dielectric matrix material must experience minimal attenuation.[24] Thus, a matrix material that exhibits low loss at optical frequencies and facilitates the fabrication of all-dielectric metamaterials is highly attractive. It is envisioned that this dielectric would be widely applicable to the fabrication of metal-dielectric metamaterials and a wide range of infrared optical devices as well.

Classically, low-loss metamaterial surfaces have been fabricated on high-index substrates (silicon, germanium, *etc.*) to avoid

aSandia National Laboratories, P.O. Box 5800, Albuquerque, NM, 87185, USA. E-mail: smdirk@sandia.gov; Tel: +505-844-7835
bCenter for Integrated Nanotechnology (CINT), Sandia National Laboratories, 1515 Eubank Blvd SE, Albuquerque, NM, 87185, USA
† Electronic Supplementary Information (ESI) available: Complete spectral data for polymer films before and after cross-linking. See DOI: 10.1039/c1jm12761f/
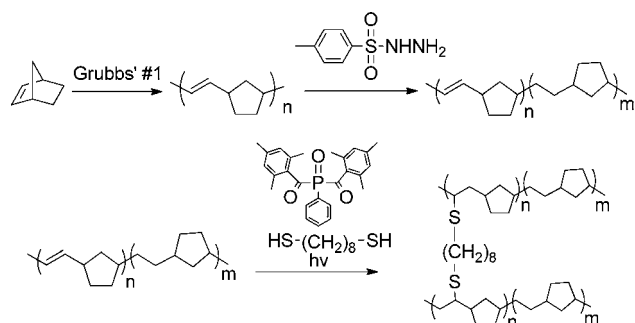
Scheme 1 Synthesis of low loss polymer matrix materials using a sequence of ROMP, hydrogenation, and thiol-ene coupling reactions.

phonon coupling and absorption.[5,25,26] High-index materials are non-ideal dielectric matrix materials because they lead to significant boundary mismatch losses, induce leakage in dielectric resonators, and increase fabrication difficulty by reducing the electrical length of the metamaterial resonators. These materials are also difficult to incorporate in the 3D constructs and require challenging polishing steps to ensure planarization. Transparent dielectrics are far more attractive but traditional low-index materials such as silicon dioxide, aluminum dioxide, and barium fluoride all exhibit strong phonon absorption modes in the thermal infrared and are equally difficult to planarize for 3D designs. Thus, the ideal dielectric matrix material for LWIR-metamaterial applications would be simultaneously low-loss, low-index, and allow for solution deposition for simple planarization. Low loss photopatternable polymer dielectrics appear to be a promising solution. However, off-the-shelf commerically available photoresist polymers also exhibit vibrational absorption bands in the optical regime.[27]

An ideal polymer dielectric would have losses comparable to polyethylene but have the additional benefits of a resist in that it is compatible with 3D fabrication techniques, photopatternable, and high temperature process tolerant.[28] We have identified a route to a tunable matrix material which satisfies each of these requirements in the thermal infrared spectral region (8–12 μm).[29,30] The materials are synthesized using the ring opening metathesis polymerization (ROMP) of norbornene followed by a partial hydrogenation to remove most of the IR absorbing olefin groups in the 8–12 μm range (Scheme 1). Photopatterning of these materials can then be achieved using the remaining olefin groups *via* a thiol-ene coupling reaction. After cross-linking, the olefin IR-absorption band is minimized and the T_g of the matrix material increases. Thus, the material is ideal for lithography and fabrication of 3D metamaterial structures operating in the LWIR spectral region. To demonstrate the low-loss nature of the matrix materials, the polymer was incorporated into an all-dielectric, infrared metamaterial. A planarizing layer of partially hydrogenated and cross-linked polynorbornene spun-cast onto etched tellurium cubes had little impact on the overall metamaterial loss.

Experimental

Reagents

All chemicals were used as received from suppliers. Norbornene (99% stabilized) and ethyl vinyl ether (99% stabilized) were

purchased from Acros organics. Grubbs' Catalyst (1st generation), *p*-toluene-sulfonylhydrazide (97%), anhydrous toluene (99.8%), 1,8-octanedithiol (97%), and phenylbis(2,4,6-trimethylbenzoyl)phosphine oxide (97%) were all obtained from Aldrich. Chloroform (HPLC grade), ethanol (ACS certified), and anhydrous *p*-xylene (ACS certified) were purchased from Fisher. Silicon wafers (single side polished, <100>) were purchased from MEMC.

Equipment

^{1}H NMR spectra were recorded on a Bruker model DRX400. GPC analysis was performed on a Polymer Labs 220 PL-GPC equipped with two columns operated in series: a PLgel 5mm MiniMIC-C (250 mm_4.6 mm) and a PLgel 5 mm MiniMIX-C (50 mm_4.6 mm) guard column. Chloroform was used as the eluent (0.4 mL min^{-1}) and the measurements were carried out at 35 °C. Calibration was performed using polystyrene standards with narrow molecular weight distributions (Fluka ReadyCal 400–2 000 000). Polymers were cast using a Gardco automatic drawdown machine or cast into thin films on silicon using a spincoater (model P6700, Specialty Coating Systems, Inc., Indianapolis IN). A Teflon® sheet was used as a substrate to cast upon for the free-standing films. UV exposure was carried out using a Lighthammer 6 (D bulb, max radiated power 350–390 nm) conveyer unit purchased from Fusion UV systems. Dynamic mechanical analysis was conducted using a TA Instruments Q800. The IR analysis was performed using a Nicolet 6700 purchased from Thermo Electron. X-ray photoelectron spectroscopy (XPS) was performed with a Kratos Axis Ultra DLD with monochromatic Al K(alpha) excitation (1486.6 eV). The analyzed spot size was 300 × 700 micrometres and chamber base pressures were less than 5 × 10^{-9} Torr. High resolution XPS was performed with the source at 150 W and the analyzer at pass energy 40, 100 meV step, and 200 ms dwell times. Counts were summed over multiple scans and charge neutralization was used to minimize peak broadening. A J. A. Woollam infrared variable angle spectral ellipsometer (IR-VASE) was used to measure the frequency-dependent complex index of refraction.

Synthesis of polynorbornene

To a 1 L Erlenmeyer flask equipped with a magnetic stir bar was added chloroform (400 mL) and norbornene (7.0 g, 74.3 mmol) and stirred until the norbornene dissolved. Next, Grubbs' #1 (0.0768 g, 0.093 mmol) was dissolved in 5 mL of chloroform and mixed into the solution of norbornene. An additional 100 mL of chloroform was added to the flask immediately after adding the catalyst to prevent gel formation. The reaction mixture was stirred for 90 min. and the catalyst was quenched with ethyl vinyl ether (4.487 mL, 46.7 mmol). Polynorbornene was slowly precipitated into ethanol (5 L), filtered, and washed with additional ethanol. The polymer was dried *in vacuo* for 12 h and isolated as a white flocculent solid (6.361 g, 91%).

Synthesis of partially hydrogenated polynorbornene

In a typical reaction, polynorbornene (1.0 g, 10.6 mmol) and tosyl hydrazide (2.5 eq.) were added to a 250 mL round bottom

This journal is © The Royal Society of Chemistry 2011

J. Mater. Chem., 2011, **21**, 13902–13908 | 13903

flask equipped with a stir bar. The flask was connected to a reflux condenser which had a stopper affixed at the top and the contents of the flask were evacuated and filled with nitrogen gas three times. While still under nitrogen, anhydrous toluene (100 mL) was added. The mixture was then heated to reflux and reacted for one hour. During this time, the tosyl hydrazide dissolved and the solution turned yellow. Upon cooling to rt, the byproducts precipitated out of solution. The partially hydrogenated polymer was precipitated into ethanol (1 liter), filtered, and washed with additional ethanol. The crude polymer was collected and purified *via* re-precipitation from toluene into ethanol. The product was dried *in vacuo* for 12 h and isolated as a white flocculent solid (0.746 g, 75%).

Polymer films and thiol-ene coupling

The polymer (0.100 g) was placed in a screw-top glass scintillation vial and dissolved in anhydrous *p*-xylene (1.5% w/v). Any particulates that did not dissolve were filtered out using a 0.45 μm PTFE filter and the solution was concentrated *in vacuo* to achieve a final concentration of 5% w/v. To this vial was added 1,8-octanedithiol (0.5 eq. relative to the olefin of the polynorbornene) and phenylbis(2,4,6-trimethylbenzoyl)phosphine oxide (0.025 eq.). The solution was stirred for 10 min and then converted into a free-standing film (approx. 20–25 μm) using draw-down technique (36 inch bar). Alternately, the polymer solution was spun-cast onto a silicon wafer (1″ × 1″, ssp) at a rate of 1000 rpm for photopatterning. Residual solvent in the film was evaporated for one hour at RT. The free-standing film was irradiated with UV light for a total exposure of 11 020 mJ cm^{-2} and subsequently dried in a vacuum oven overnight at 50 °C.

Results and discussion

Polymer synthesis

The synthesis of polynorbornene was carried out using ROMP with Grubbs' 1st generation catalyst (Scheme 1).[31] The reaction is known to be both facile and high yielding while also allowing for the molecular weight to be controlled simply by varying the catalyst to monomer ratio. Preliminary experiments shown that a molecular weight (Mw) of ~75 000 was most ideal for the subsequent hydrogenation reactions compared to lower (50 000) and higher (125 000) molecular weights. Thus, normal reaction conditions were employed to yield polynorbornene (quant.) as confirmed by proton nuclear magnetic resonance spectroscopy (¹H NMR), and the polymer Mw was measured to be 87 088 relative to narrow molecular weight polystyrene standards using gel permeation chromatography (GPC).

Polynorbornene is a highly unsaturated polymer so it is quite prone to oxidative degradation and inherently limited when it comes to solubility in organic solvents. In an effort to identify the most process-friendly and optimal photopatternable IR matrix material, the olefin content was removed by hydrogenating the polymer to varying degrees. Each hydrogenation reaction was conducted using tosyl hydrazide as the diimide hydrogenation precursor (Scheme 1).[32,33] The hydrazide undergoes decomposition at elevated temperatures to form diimide (the reactive species) as well as *p*-toluenesulfinic acid and bis(*p*-tolyl) disulfide
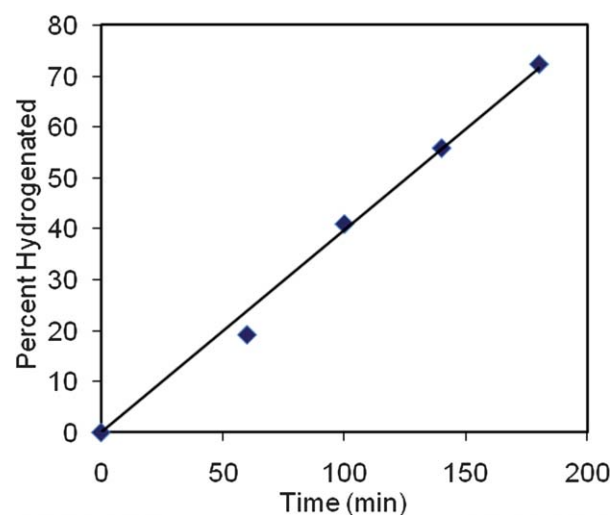

Fig. 1 Percent hydrogenated *vs.* time.

by-products. The advantages of this reaction are that the degree of hydrogenation can be controlled by altering the reaction time or reaction stoichiometry and the by-products can easily be removed during workup by precipitation into ethanol. Furthermore, the degree of hydrogenation is determined using ¹H NMR by simply integrating the methine peaks between 5–5.5 ppm and the methylene peaks between 0.5–3 ppm.

Several polymer matrix materials were prepared by reacting 2.5 eq. of the hydrogenating agent with polynorbornene for 60–180 min. A linear correlation was observed between the percent hydrogenation *versus* reaction time (Fig. 1) which was found to be both reproducible and high-yeiding. Each of the four partially hydrogenated polynorbornene samples were soluble in nonpolar solvents (toluene, xylene, chloroform) to varying degrees. Partially hydrogenating to 18.2% led to improved solubility over non-hydrogenated polynoroborbene but solubility decreased slightly as more olefin was removed (72%). This is probably due to a shift in the amorphous behavior of the polymer as a larger percentage of the olefin is removed.[34] Nonetheless, the hydrogenated polymer materials were of superior solubility compared to polynorbornene and the reaction time allowed for excellent control of the hydrogenation step.

Thiol-ene coupling and optimization

Each of the partially hydrogenated samples were cross-linked using the thiol-ene reaction (Scheme 1). This is a type of click reaction which takes advantage of weak sulfur-hydrogen bonds in thiols and reactive carbon-carbon bonds.[35] On addition of photoinitiator and subsequent UV exposure, the reaction proceeds *via* free radical mechanism to rapidly generate uniform polymer networks in high quantitative yield. In a typical reaction, the partially hydrogenated polymer was dissolved in anhydrous *p*-xylene (5% w/v) and 1,8- octanedithiol (0.50 eq. relative to the olefin of the polynorborne) was added as the crosslinker.[36] A small amount of bisacylphosphine oxide (BAPO) photoinitiator (0.025 eq) was then mixed into the reaction vial and a free-standing film (20–25 μm thick) was cast from this solution using draw-down technique. All of the films prepared in
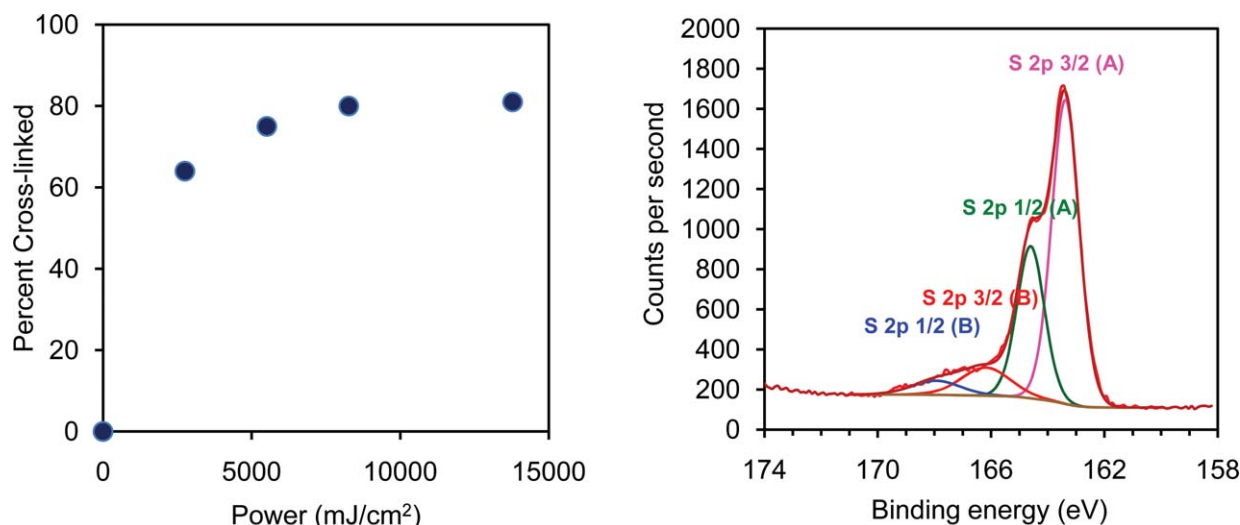
Fig. 2 A 25 μm thick film cast from a solution containing polynorbornene, 1,8-octanedithiol, and BAPO exposed to light at different intervals to induce cross-linking (left) and analyzed using XPS analysis after cross-linking (right).

this manner were subsequently irradiated with a Lighthammer UV conveyer unit (D bulb) to induce cross-linking. Alternatively, irradiation could be carried out using a UV lamp.

The extent of cross-linking was optimized first by measuring the amount of light necessary to crosslink non-hydrogenated polynorbornene *via* the thiol-ene reaction. A free-standing film approximately 25 μm thick was cast and exposed to UV light at increments of 565 mJ cm^{-2}. The amount of cross-linked olefin was determined using IR analysis by integrating the methine peak (966 cm^{-1}) *versus* the broad methylene peak (2800–3100 cm^{-1}).[37] Though this method is somewhat skewed by the presence of additional methylene groups from the 1,8-octanedithiol, a reasonable correlation was observed in a plot of the percent cross-linked *versus* exposure power (Fig. 2). The majority of the cross-linking occurred within ~5000 mJ cm^{-2}. Beyond this point, cross-linking gradually increased until plateauing at a maximum value of 81%. Additional exposures did

not lead to more highly cross-linked films. This is probably due to a lack of mobility and/or alignment of the unreacted olefin and thiol for the thiol-ene reaction. Nonetheless, the optimum amount of power required for maximum cross-linking was identified to be 11 020 mJ cm^{-2}.

High resolution X-ray photoelectron spectroscopy (XPS) analysis was also used to confirm cross-linking in the exposed sample (Fig. 2). Two distinct sulfur environments were observed with the primary component assigned as bound sulfur ($S_{2p3/2}$ binding energy of 163.4 eV) and a smaller secondary component assigned as that of unbound sulfur ($S_{2p3/2}$ binding energy of 166.2 eV).[38] The ratio of bound *versus* unbound is consistent with the IR data and suggests that, though a minimal amount of unbound thiol remained in the film due to incomplete cross-linking, the majority reacts to form new sulfur-carbon linkages *via* the thiol-ene reaction thereby eliminating most of the olefin absorption in the 8–12 μm spectral region.
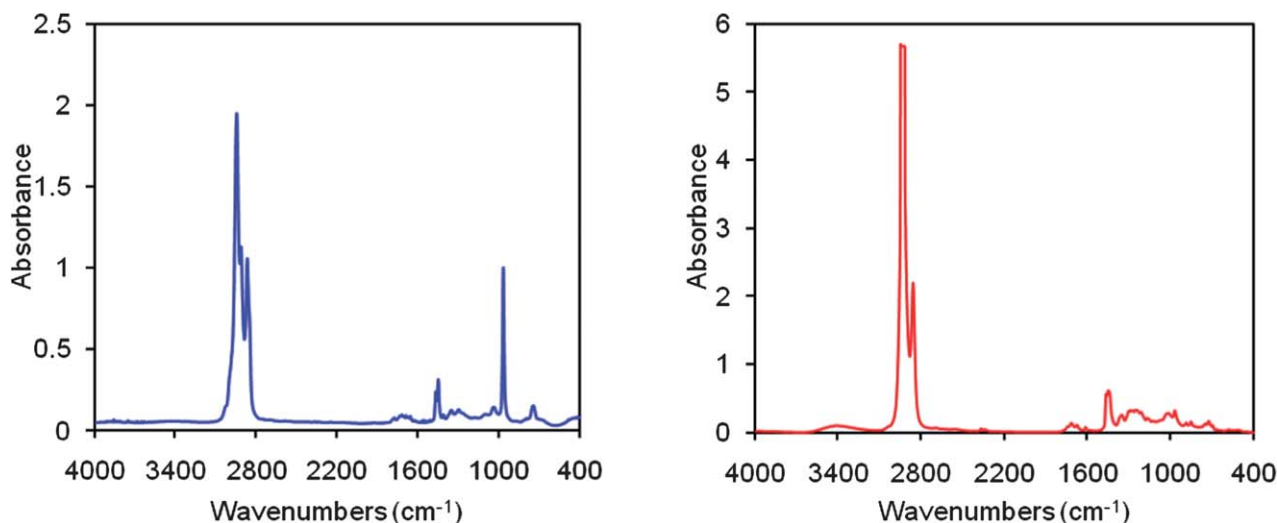
Fig. 3 FTIR spectra for free-standing films (20–25 μm thick) consisting of partially hydrogenated polynorbornene (18.2%) before and after cross-linking (blue and red line respectively).

Table 1 Influence of the thiol-ene coupling reaction on the T_g

Entry	Percent Hydrogenated	T_g [°C][a]	Cross-linked
1	0	44	
2	0	115	√
3	18.2	34	
4	18.2	49, 101	√
5	41.0	36	
6	41.0	42, 95	√
7	55.9	23	
8	55.9	35, 71	√
9	72.4	27	
10	72.4	27, 54	√

[a] Measured using DMA analysis for free-standing films (20–25 μm). The value was recorded from the peak of the tan delta.

### FTIR and thermal analysis

The partially hydrogenated polymers should be more amenable to LWIR-metamaterial applications because of the lower IR- absorbing olefin content and good solubility. The remaining olefin could be reduced even further *via* the thiol-ene reaction to yield materials that are not only more optically favorable, but thermally favorable as well. To demonstrate this, two free-standing films were cast for each partially hydrogenated polymer. One of the films was subjected to the thiol-ene reaction whereas the second film was a control which contained only the partially hydrogenated pre-polymer. IR analysis was carried out on each of the films to reveal that olefin absorbance had in fact decreased in the cross-linked films. For example, a considerable reduction in the methine peak at 966 cm^{-1} was observed for an irradiated film prepared from partially hydrogenated (18.2%) polynorbornene (Fig. 3).[39]

The thermal properties of the films were characterized next using dynamic mechanical analysis (DMA).[40] The cross-linked materials should be more thermally stable than their non cross-linked counterparts due to an increase in density within the polymer matrix. Indeed, the T_g temperatures (Table 1) for the control films were low (23–44 °C) compared to those cross-linked using the thiol-ene reaction (T_g = 54–115 °C). Cross-linked polynorbornene was found to be the most thermally stable of all the exposed films (T_g = 115 °C), whereas films prepared from more extensively hydrogenated polynorbornene showed only a marginal increase in T_g. This is best explained by the lower availability of olefin in the extensively hydrogenated polymer. In most cases, two tan delta peaks were observed which is attributed to a small amount of unreacted olefin. Considering the DMA results along with the FTIR data, the least hydrogenated polynorbornene sample (18.2%) appears to be the optimum material for LWIR-metamaterial applications as it provides an excellent combination of solubility, thermal stability, and minimized absorption in the 8–12 μm spectral region.

Ellipsometry

A J. A. Woollam infrared variable angle spectral ellipsometer (IR-VASE) was used to measure the frequency-dependent complex index of refraction for partially hydrogenated polynorbornene (18.2%) that was cross-linked *via* the thiol-ene reaction. Extraction of the optical properties was carried out *via* a general thin-film measurement procedure previously described by Woollam *et al.*[41] The polymer was first spun onto a substrate consisting of a 1 inch square of 380 μm thick silicon coated with an optically-thick layer of aluminum. The aluminum layer was required to prevent the polymer film from acting as an anti-reflective coating for the bare silicon. The IR-VASE was fixed to an operating spectral range of 2–25 μm and angle of incidences of 55 degrees to 70 degrees with a step size of 5 degrees. The measured ellipsometric constants, Ψ and Δ, were fit to a series of Gaussian oscillators centered at energies corresponding to the film's vibrational modes using Wollam's WVASE software.[42] Extracted optical properties are shown in Fig. 4 for a 1.645 μm thick spin-cast film. The measured loss over the integrated 8–12 μm is significantly less than comparable polymers typically
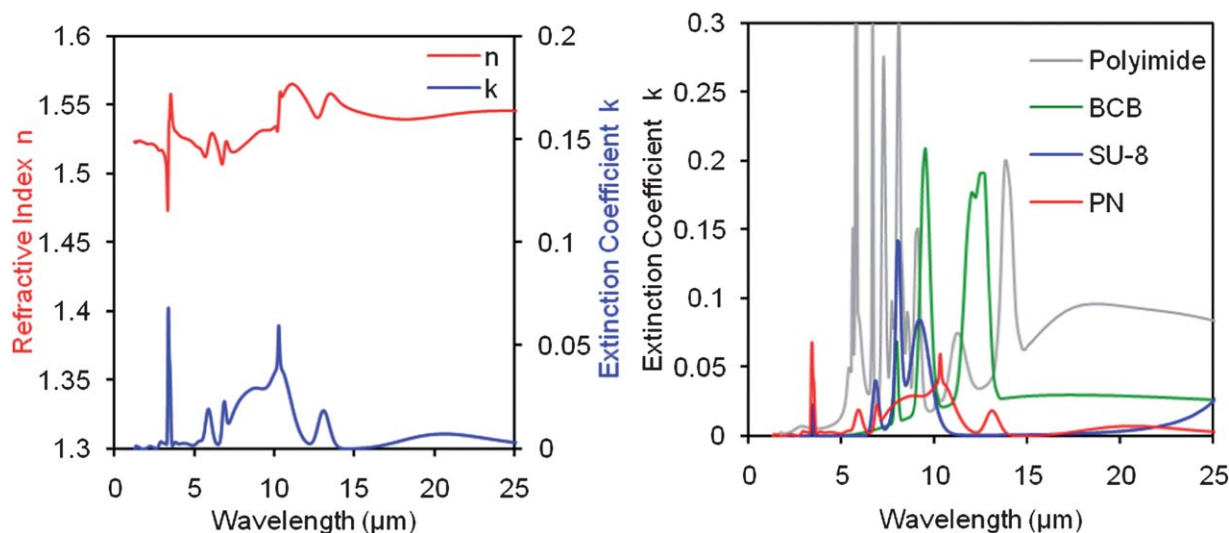
Fig. 4 The experimentally measured complex refractive index and extinction coefficient for partially hydrogenated polynorbornene (18.2%) cross-linked using the thiol-ene reaction. The extinction coefficient for the cross-linked polynorbornene sample (PN) is significantly less than that of other commercially available photoresists that have been cross-linked.
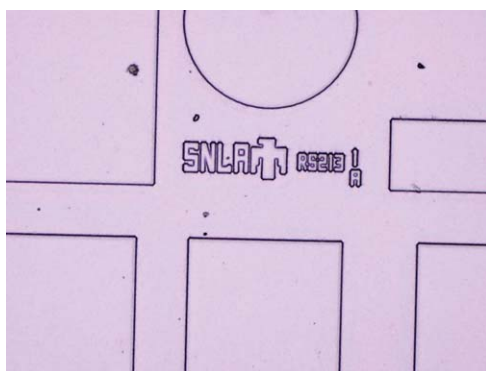
Fig. 5 Optical microscope image of photopatterned low loss LWIR-metamaterial matrix.

used in microfabrication such as polyimide and benzocyclobutene based polymer (BCB).[27]

Photopatterning

The optimal polymer material was tested next for microfabrication compatibility. Preliminary experiments determined that an adhesion layer was required to ensure that thick films (>1 μm) remained adhered to the silicon substrate during UV exposure. The adhesion layer was deposited by spin casting a layer of non-hydrogenated polynorbornene containing dithiol and photocross-linking *via* thiol-ene reaction to generate a thin film (28 nm). Next, a solution of partially hydrogenated polynorbornene (18.2%), cross-linker, and photoinitiator was prepared under the same conditions used to make the free-standing films and spun cast onto the wafer (see experimental). The film was irradiated (405 nm, 20 mW cm^{-2}) using a mask aligner at a total power of 6,000 mJ cm^{-2}. The film was then developed in toluene for 5 min to remove the non cross-linked polymer and maintain the exposed regions. Though development in toluene was somewhat difficult to observe since the polymer

and toluene have a similar index of refraction (n_D^{22} 1.5), photopatterned structures with well-refined micron-sized features were evident throughout the film (Fig. 5).

Dielectric resonator loss

The impact of the optimum polymer material on the overall loss of an all-dielectric, infrared metamaterial was evaluated next.[43] Briefly, an optically thick layer of tellurium (1.7 μm) was deposited on a barium fluoride substrate and patterned using standard e-beam lithography and a reactive ion etching process. The optimum partially hydrogenated polymer was spun-cast onto the etched tellurium wafer and photochemically cross-linked using the thiol-ene reaction. A cross-section image of the wafer taken using scanning electron microscopy (SEM) shown that the polymer had good planarization and flat-top surface behavior (Fig. 6). More importantly, the polymer had little impact on the overall loss of the metamaterial as transmission spectra collected both in the absence and presence of polymer were marginally different (Fig. 6). As expected, the addition of the polymer to the wafer led to an upward shift in wavelength for both electric and magnetic resonances. This is due to an overall increase in the permittivity/refractive index of the resonator system. Finally, an absorption feature was observed at 10.3 μm which is consistent with the peak in the measured extinction coefficient for blanket polynorbornene film. This peak is associated with a small amount of unreacted olefin remaining in the polymer. Ultimately, though, the polymer had little influence on the overall metamaterial loss due to a lack of strong absorptions in the 8–12 μm spectral range. This is in contrast to commercially available photopatternable polymers that have much higher losses.[22,27]

Conclusions

In summary, novel low loss photopatternable polymer dielectric materials were synthesized by partially hydrogenating polynorbornene to varying degrees and using the thiol-ene coupling
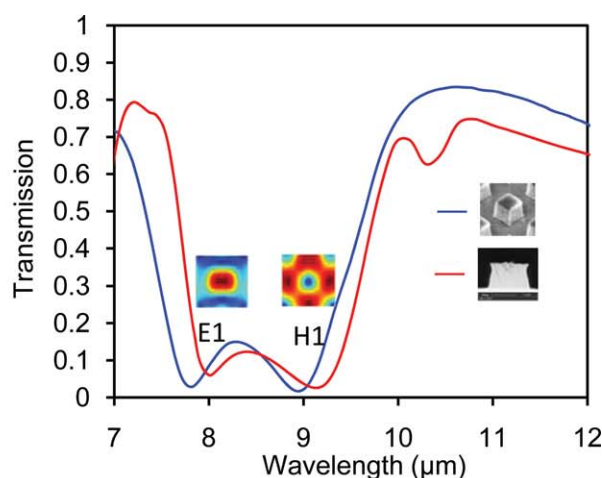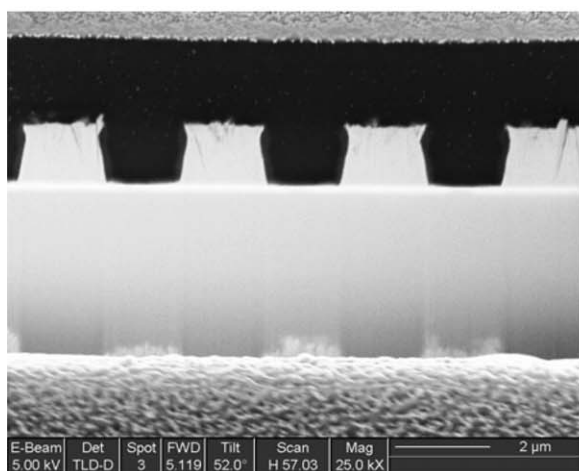
Fig. 6 Cross-section view of an all-dielectric infrared metamaterial taken using SEM (left) and transmission spectra for the same metamaterial before and after adding the optimum polymer material (right). The polymer, shown in black in the SEM has a flat surface and planarizes well over etched tellurium cubes. Though the electric resonance (E1) and magnetic resonance (H1) shifts to a slightly higher wavelength when the polymer is present (red line), there is minimal attenuation of the resonant fields overall.

This journal is © The Royal Society of Chemistry 2011

J. Mater. Chem., 2011, **21**, 13902–13908 | **13907**

reaction to cross-link the remaining olefin groups. The material characteristics were measured using FTIR and DMA analysis from free-standing films, and the optical constants of spun-cast films were characterized using IR-VASE. A 1.6 μm thick layer of photopatterned material was demonstrated using the optimum partially hydrogenated polymer (18.2%). An overcoat layer of the low loss polymer on an all-dielectric, infrared metamaterial had excellent planarization and little impact on the overall loss of the metamaterial. The thermal and spectral properties of these matrix materials suggests they are ideal components for fabricating LWIR-metamaterials and other applications that require a low loss negative photoresist.

Acknowledgements

Notes and references

1 V. G. Veselago, *Sov. Phys. Usp.*, 1968, **10**, 509–514.
2 R. A. Shelby, D. R. Smith and S. Schultz, *Science*, 2001, **292**, 77–79.
3 J. B. Pendry, *Phys. Rev. Lett.*, 2000, **85**, 3966–3969.
4 D. Schurig, J. J. Mock, B. J. Justice, S. A. Cummer, J. B. Pendry, A. F. Starr and D. R. Smith, *Science*, 2006, **314**, 977–980.
5 T. J. Cui, D. R. Smith and R. Liu, in *Metamaterials Theory, Design, and Applications* Springer, New York, 2010.
6 V. M. Shalaev, W. S. Cai, U. K. Chettiar, H. K. Yuan, A. K. Sarychev, V. P. Drachev and A. V. Kildishev, *Opt. Lett.*, 2005, **30**, 3356–3358.
7 S. Zhang, W. J. Fan, N. C. Panoiu, K. J. Malloy, R. M. Osgood and S. R. J. Brueck, *Phys. Rev. Lett.*, 2005, **95**, 137404.
8 G. Dolling, C. Enkrich, M. Wegener, C. M. Soukoulis and S. Linden, *Opt. Lett.*, 2006, **31**, 1800–1802.
9 G. Dolling, M. Wegener, C. M. Soukoulis and S. Linden, *Opt. Lett.*, 2007, **32**, 53–55.
10 S. P. Burgos, R. de Waele, A. Polman and H. A. Atwater, *Nat. Mater.*, 2010, **9**, 407–412.
11 C. M. Soukoulis, S. Linden and M. Wegener, *Science*, 2007, **315**, 47–49.
12 V. M. Shalaev, *Nat. Photonics*, 2007, **1**, 41–48.
13 S. A. Ramakrishna and J. B. Pendry, *Phys. Rev. B*, 2003, **67**, 201101.
14 S. M. Xiao, V. P. Drachev, A. V. Kildishev, X. J. Ni, U. K. Chettiar, H. K. Yuan and V. M. Shalaev, *Nature*, 2010, **466**, 735–738.
15 D. B. Burckel, J. R. Wendt, G. A. Ten Eyck, A. R. Ellis, I. Brener and M. B. Sinclair, *Adv. Mater.*, 2010, **22**, 3171–3175.
16 J. Valentine, S. Zhang, T. Zentgraf, E. Ulin-Avila, D. A. Genov, G. Bartal and X. Zhang, *Nature*, 2008, **455**, 376–379.
17 L. Lewin, *Proc. Inst. Electr. Eng.*, 1947, **94**, 65–68.
18 I. Vendik, O. Vendik, I. Kolmakov and M. Odit, *Opto-Electron. Rev.*, 2006, **14**, 179–186.
19 Q. Zhao, J. Zhou, F. L. Zhang and D. Lippens, *Mater. Today*, 2009, **12**, 60–69.
20 C. L. Holloway, E. F. Kuester, J. Baker-Jarvis and P. Kabos, *IEEE Trans. Antennas Propag.*, 2003, **51**, 2596–2603.
21 Q. Zhao, L. Kang, B. Du, H. Zhao, Q. Xie, X. Huang, B. Li, J. Zhou and L. Li, *Phys. Rev. Lett.*, 2008, **101**, 027402.
22 J. C. Ginn, G. A. Ten Eyck, I. Brener, D. W. Peters and M. B. Sinclair, in *OSA Technical Digest*, Optical Society of America, Tuczon, AZ, 2010, p. MWD2.
23 J. C. Ginn, D. W. Peters, J. R. Wendt, J. O. Stevens, P. F. Hines, I. Brener, L. I. Basilio, L. K. Warne, J. F. Ihlefeld, P. G. Clem and M. B. Sinclair, unpublished work.
24 D. J. Shelton, I. Brener, J. C. Ginn, M. B. Sinclair, D. W. Peters, K. R. Coffey and G. D. Boreman, *Nano Lett.*, 2011, **11**, 2104–2108.
25 W. Cai and V. Shalaev, in *Optical Metamaterials Fundamentals and Applications* Springer, New York, 2010.
26 N. Engheta and R. W. Siolkowski, ed., in *Metamaterials: Physics and Engineering Explorations*, Wiley-IEEE Press, Piscataway, NJ, 2006.
27 W. R. Folks, J. Ginn, D. Shelton, J. Tharp and G. Boreman, *Phys. Status Solidi C*, 2008, **5**, 1113–1116.
28 A. Boltasseva and V. M. Shalaev, *Metamaterials*, 2008, **2**, 1–17.
29 R. D. Rasberry, Y.-J. Lee, J. C. Ginn, P. Hines, C. L. Arrington, M. B. Sinclair, P. G. Clem, A. E. Sanchez and S. M. Dirk, presented in part at the 2010 Materials Research Society Fall Meeting, Boston, MA, M10.19. http://www.mrs.org/f10-abstract-m/ (accessed May 25, 2011).
30 R. D. Rasberry, Y.-J. Lee, J. C. Ginn, P. Hines, C. L. Arrington, A. E. Sanchez, M. B. Sinclair, S. M. Dirk, *PMSE Proceedings of the 241st ACS National Meeting and Exposition, Anaheim, CA, USA*, 2011http://pubs.acs.org/cgi-bin/preprints/display?div=pmse&meet=241&page=64508_13244.pdf (accessed May 25, 2011).
31 R. H. Grubbs, in *Handbook of Metathesis*, Wiley-VCH, Weinheim, 2003.
32 F. Cataldo, *Polym. Int.*, 1994, **34**, 49–57.
33 L. A. Mango and R. W. Lenz, *Makromol. Chem.*, 1973, **163**, 13–36.
34 L. B. W. Lee and R. A. Register, *Macromolecules*, 2005, **38**, 1216–1222.
35 C. E. Hoyle and C. N. Bowman, *Angew. Chem., Int. Ed.*, 2010, **49**, 1540–1573.
36 Prior to adding the cross-linker, the polymer solution was diluted to 1.5%, filtered using a 0.45 μm PTFE filter, and concentratred to 5% w/v in order to removed any undissolved polymer particles.
37 The polymer backbone is comprised of *trans* double bonds which absorb at 966 cm^{-1} and *cis* double bonds which absorb at 740 cm^{-1} with the the *trans* being the more predominate of the two. For more information, please refer to ref. 32.
38 D. G. Castner, K. Hinds and D. W. Grainger, *Langmuir*, 1996, **12**, 5083–5086.
39 See supplemental for complete spectral data.
40 L. E. Nielsen and R. F. Landel, *Mechanical Properties of Polymers and Composites*, Marcel Dekker, New York, 1994.
41 J. A. Woollam, B. Johs, C. M. Herzinger, J. N. Hilfiker, R. Synowicki and C. L. Bungay, *SPIE Proc.*, 1999, **CR72**, 3–28.
42 D. D. Meneses, M. Malki and P. Echegut, *J. Non-Cryst. Solids*, 2006, **352**, 5301–5308.
43 The fabrication of the metamaterial is being discussed elsewhere. See ref. 23.